# X-ray magnetic circular dichroic spectrum at the *K* edge of the transition metal in *R-T* intermetallics and its relationship with the magnetism of the rare earth

M. A. Laguna-Marco,[1] C. Piquer,[2] and J. Chaboy[3]

[1]*Advanced Photon Source, Argonne National Laboratory, Argonne, Illinois 60439, USA*
[2]*Instituto de Ciencia de Materiales de Aragón and Departamento de Ciencia y Tecnología de Materiales y Fluidos, CSIC–Universidad de Zaragoza, 50009 Zaragoza, Spain*
[3]*Instituto de Ciencia de Materiales de Aragón and Departamento de Física de la Materia Condensada, CSIC–Universidad de Zaragoza, 50009 Zaragoza, Spain*

We present here a study of the x-ray magnetic circular dichroism (XMCD) at the *K* edge of the transition metal on rare-earth (*R*) transition-metal (*T*) intermetallics. The analysis of the *T* *K*-edge XMCD in the $RT_2$ compounds ($T=$Fe,Co) reveals that, when *R* is magnetic, there is a rare-earth contribution to these spectra which is as intense as to dominate the overall shape and sign of the XMCD signal. As a result, for a given *R*, the XMCD signal recorded in $R$Fe$_2$ is very similar to that of $R$Co$_2$ despite the magnitude of the Co $3d$ magnetic moment is quite different from that of Fe in these compounds. The study of XMCD$_R$ as a function of the rare earth itself suggests that the rare-earth contribution to the *T* *K*-edge XMCD has an orbital origin and that its magnitude is related to the orbital component of the magnetic moment, $L_{4f}$, instead of the total magnetic moment. Moreover, despite no significant variation in the signals is found when Fe is changed by Co, the amplitude of the signals decreases remarkably as Fe or Co are diluted by nonmagnetic Al. Since aluminum substitution affects only slightly the magnitude of the individual $\mu_T$ and $\mu_R$ magnetic moments but strongly reduces the exchange interaction, this points out that XMCD$_R$ shows also a dependence on the strength of the *R-T* interaction. Therefore, our results suggest that the behavior of XMCD$_R$ can be accounted for in terms of a "molecular fieldlike" (with $B_{RT} \propto n_{RT} L_R$) model.

PACS number(s): 78.70.Dm, 71.20.Lp, 75.50.Bb, 75.50.Cc

## I. INTRODUCTION

X-ray magnetic circular dichroism (XMCD) has attracted much interest in the last years as a useful tool to investigate magnetic states by incorporating the element specificity inherent to core-level spectroscopies.[1–4] This peculiarity allows one to probe separately contributions from various magnetic elements in a single magnetic material.[5–10] Alongside the experimental progress, the theoretical understanding of XMCD, based on both a localized and itinerant picture, has also considerably advanced.[11] In particular, the derivation of the so-called sum rules,[12,13] showing the relationship between the integrated XMCD signals for given spin-orbit-split absorption edges and the ground state orbital and spin magnetic moments, is one of the keystones for applying XMCD to basic and applied research on magnetism.

Nowadays, XMCD is commonly used to probe the spin and orbital magnetic moments for those cases in which the final states are localized such as the $L_{2,3}$ edges of $3d$ transition metals and the $M_{4,5}$ edges of lanthanides and actinides. Nevertheless, the same does not hold for cases in which the final state is delocalized such as the 4p states of the transition metals probed by the *K* edge. Initially, the *K*-edge XMCD was thought to be proportional to the *p*-projected spin density of states.[6] While in the case of bcc Fe the XMCD *K*-edge spectrum is well described by spin-polarized relativistic multiple-scattering computations,[14,15] this interpretation fails for the Co and Ni systems.[16–18] Later, Igarashi and Hirai concluded that the XMCD at the *K* edge of the ferromagnetic metals Fe, Co, and Ni, comes from the 4p orbital polarization induced by the mixing to the 3d states at neighboring sites.[19,20] These authors stated that the shape of the XMCD spectrum near the *K* edge is determined by the 3d-projected orbital magnetization density of states (ODOS). These and subsequent works have proposed a magneto-optical sum rule connecting the *K*-edge XMCD with the *p*-projected orbital magnetization density of unoccupied states.[19–25]

The above cited analysis indicates that the relationship between the Fe *K*-edge XMCD spectra and the local magnetic moments is limited to the orbital magnetization. However, a definitive answer about the origin of the XMCD spectrum at the *K* edge is still missing. It is worth noticing at this point that in the absorption process at the *K* edge of transition metals the core electron enters the 4p states, which are not the states constituting the magnetic order of the *T* atoms. The XMCD signal of the 4p states emerges due to the 4p orbital polarization induced by the mixing with the 3d states, so that the *K*-edge XMCD signal is an indirect probe of the magnetism of the transition metal. And the above scenario becomes more complicated in those cases where more than one magnetic element is present, as in the *R-T* intermetallic compounds. Previous works[26–31] have shown that the *T* *K*-edge spectrum in these cases is also affected by the presence of the *R* sublattice. These works indicate that there is a contribution to the XMCD coming from the 4p polarization induced by the hybridization with the $R(5d)$ states and that this extra signal reflects the magnetization of the rare-earth sublattice. However, the detailed descriptions of the effect of *R* on the polarization of the $T(4p)$ states and the relationship between the *T* *K*-edge XMCD spectrum and the *R* magnetism is still missing. The question arising is what information on the magnetic properties of the systems under

study can be derived from the analysis of the $K$ edge. Answering this question can be of particular significance not only for $R$-$T$ intermetallics but also in the case of systems in which the magnetism is not associated to localized states but to conduction band effects, as for example the magnetism due to the charge transfer that takes place upon surface functionalization of nanoparticle systems.

The present work is aimed to get a deeper insight into the interpretation of the $T$ $K$-edge XMCD spectra in rare-earth transition-metal ($R$-$T$) intermetallic compounds and explore what the $K$-edge XMCD tells us about the magnetism of these multicomponent magnetic materials. To this end we have performed a study of the $T$ $K$ edge in the ferromagnetic $R(Al_{1-x}Fe_x)_2$ and $R(Al_{1-x}Co_x)_2$ series ($x=0.25-1$). In a first step, we study the binary $RT_2$ compounds ($T=Fe,Co$). Our results show that in the case of the $RT_2$ compounds there is a huge rare-earth contribution to the $T$ $K$-edge XMCD spectra, $XMCD_R$, which dominates the amplitude and spectral shape of the XMCD signal recorded at the $T$ $K$ edge. The next step in this study is to get a deeper insight into the origin of this $XMCD_R$ contribution and how it relates to the magnetic state of the rare earth. To this end we carry out several studies in which the XMCD spectrum at the $T$ site is monitored as a function of different parameters: (i) for several selected $R$-$T$ compounds, the variation in the XMCD when the temperature increases from 5 to 300 K is analyzed; (ii) the behavior of the $T$ $K$-edge XMCD upon decreasing the Fe content is studied; and (iii) the dependence on the specific rare earth in the alloy is monitored.

## II. EXPERIMENTAL

Polycrystalline $R(Al_{1-x}Fe_x)_2$ samples (with $R=$ Gd, Tb, Dy, Ho, Lu, and Y; $x=1$, 0.75, 0.50, and 0.25) and $R(Al_{1-x}Co_x)_2$ samples [with $R=$ Pr, Nd, Gd, Tb, Dy, Ho, Er, Lu, and Y; $x=1$ but in the cases of Y ($x=0.85$) and Lu ($x=0.90$)] were prepared by arc melting in an argon atmosphere according to standard methods.[32] Regarding the iron Laves phases with Nd and Pr, the synthesis of these samples is only possible under high pressure conditions[33] and no works have been reported about the magnetic properties of these compounds. This hindrance has prevented us from including NdFe$_2$ and PrFe$_2$ in our study. The as-cast alloys were wrapped in Ta foil and enclosed in silica tubes, under Ar gas. Compounds were annealed at 800 °C for 72 h and then quenched to room temperature. X-ray diffraction analyses indicate that all the samples show the MgCu$_2$-type (C15) Laves structure, with the exception of compounds with $x=0.5$ which crystallize in the hexagonal MgZn$_2$-type (C14) structure. The presence of secondary phases is less than 5% overall, in all the cases. The macroscopic magnetic measurements, $M(T)$ and $M(H)$, were recorded by using a commercial superconducting quantum interference device magnetometer (Quantum Design MPMS-S5). For temperatures above $T=300$ K, $M(T)$ measurements were recorded by using a Faraday-type balance. The Curie temperature $T_C$ was obtained from the inflection point of the $M(T)$ curves. The detailed structural and magnetic characterization of the samples can be found in Ref. 32.

XMCD experiments were performed at the beamline BL39XU of the SPring8 Facility.[34] XMCD spectra were recorded in the transmission mode at the $K$ edge of the transition metal by using the helicity-modulation technique.[35] The sample is magnetized by an external magnetic field applied in the direction of the incident beam and the helicity is changed from positive to negative each energy point. XMCD spectra were recorded at different temperatures and under the action of different applied magnetic fields. The energy resolution is 0.5 eV. Recording one XMCD spectrum took 30 min. In all the cases, the origin of the energy scale was chosen at the inflection point of the absorption edge and the XAS spectra were normalized to the averaged absorption coefficient at high energy ($\sim 60$ eV above the edge). The XMCD spectrum was obtained as the difference of the absorption coefficient $\mu_c=(\mu^- - \mu^+)$ for antiparallel, $\mu^-$, and parallel, $\mu^+$, orientation of the photon helicity and the magnetic field applied to the sample. For sake of accuracy the direction of the applied magnetic field is reversed and XMCD, now $\mu_c=(\mu^+ - \mu^-)$, is recorded again by switching the helicity. The subtraction of the XMCD spectra recorded for both field orientations cancels, if present, any spurious signal. It should be noted that by using this definition of the XMCD, the sign of the signals hereafter is referred to the direction of the total magnetization of each compound.

## III. RESULTS AND DISCUSSION

### A. Fe vs Co $K$-edge XMCD in $RT_2$: Influence of the $R$ contribution

The XMCD spectra at the transition-metal $K$ edge of the Laves compounds in which $R$ is nonmagnetic, Y or Lu, are shown in Figs. 1(a) and 1(b). In the case of the iron series, the XMCD spectra correspond to the binary compounds YFe$_2$ and LuFe$_2$, whereas in the cobalt series, Y(Al$_{0.15}$Co$_{0.85}$)$_2$ and Lu(Al$_{0.1}$Co$_{0.9}$)$_2$ are shown. It is worth mentioning here that within the $R$Fe$_2$ series all the compounds, including YFe$_2$ and LuFe$_2$, show ferro (or ferri) magnetism, with $\mu_{Fe} \sim 1.5\mu_B$. By contrast, in the $R$Co$_2$ series, YCo$_2$ and LuCo$_2$ are Pauli paramagnets, whereas $R$Co$_2$ compounds with magnetic heavy $R$ are ferrimagnets with a magnetic moment for Co $\mu_{Co} \sim 0.8\mu_B$. Therefore, YCo$_2$ and LuCo$_2$ compounds are not good candidates to analyze the behavior of the $K$ Co XMCD signal in absence of a magnetic rare earth. On the other hand, the substitution of Co by nonmagnetic Al induces ferromagnetic order.[36–40] Within the Y(Al$_{1-x}$Co$_x$)$_2$ and Lu(Al$_{1-x}$Co$_x$)$_2$ series, the maximum spontaneous Co magnetic moment, derived from the value of the magnetization at 10 T (5 T), is $\mu_{Co}=0.3(0.2)\mu_B$ and $0.7(0.6)\mu_B$ for Y(Al$_{0.15}$Co$_{0.85}$)$_2$ and Lu(Al$_{0.1}$Co$_{0.9}$)$_2$, respectively.[32] Hence, we have chosen these compounds to analyze the behavior of the $K$ Co XMCD signal when a nonmagnetic rare earth is present.

These spectra are compared to those of reference metal foils: bcc Fe and hcp Co. The Fe $K$-edge XMCD spectra of YFe$_2$ and LuFe$_2$ are quite similar to that of Fe metal [see Fig. 1(a)]. They all show a main narrow positive peak (A) at the absorption threshold. For higher energies, bcc Fe shows a negative dip ($\sim 12$ eV wide), while in the case of YFe$_2$ and
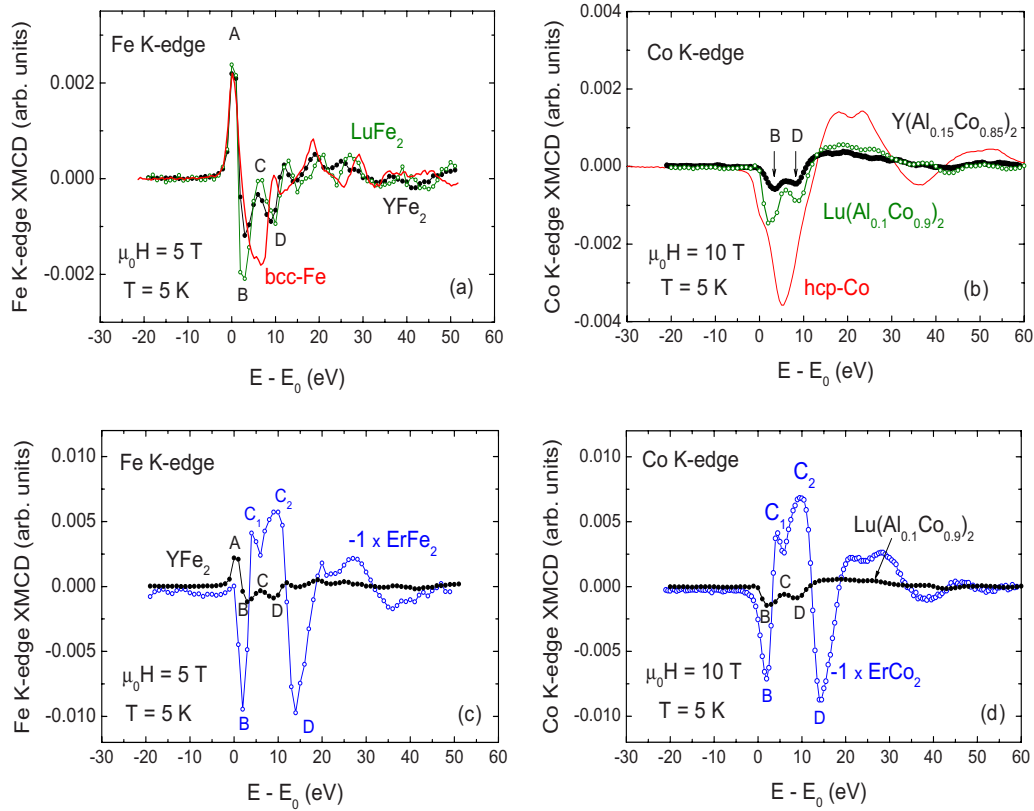
FIG. 1. (Color online) (a) Comparison of the normalized Fe $K$-edge XMCD spectra of YFe$_2$ (black, ●), LuFe$_2$ (green, ○) and bcc Fe (red, solid line). (b) Comparison of the normalized Co $K$-edge XMCD spectra of Y(Al$_{0.15}$Co$_{0.85}$)$_2$ (●), Lu(Al$_{0.1}$Co$_{0.9}$)$_2$ (green, ○) and hcp Co (red, solid line). (c) Comparison of the normalized Fe $K$-edge XMCD spectra of ErFe$_2$ (blue, ○) and YFe$_2$ (●). The sign of the ErFe$_2$ signal has been reversed accordingly to the sign of the Fe magnetization in the ferromagnetic YFe$_2$ compound (see text for details). (d) Comparison of the normalized Co $K$-edge XMCD spectra of ErCo$_2$ (blue, ○) and Lu(Al$_{0.1}$Co$_{0.9}$)$_2$ (●). The sign of the ErCo$_2$ spectrum has been reversed (see text for details).

LuFe$_2$ a small positive peak C emerges superimposed to the negative dip. As a result, the XMCD spectrum shows two negative narrow peaks B and D located at ∼3 and 9 eV above the edge, respectively. Figure 1(b) shows the comparison of the normalized Co $K$-edge XMCD spectra of Y(Al$_{0.15}$Co$_{0.85}$)$_2$, Lu(Al$_{0.1}$Co$_{0.9}$)$_2$ and hcp Co. Roughly speaking, the profile of the three spectra is similar, consisting of a broad negative dip. However, in the Co $K$-edge XMCD spectra of Y(Al$_{0.15}$Co$_{0.85}$)$_2$ and Lu(Al$_{0.1}$Co$_{0.9}$)$_2$ two peaks, B and D, at the same energy as in YFe$_2$, can be distinguished. The main difference between the Fe and Co $K$-edge XMCD lies at $E-E_0 \sim 0$ eV. The Co $K$ edge does not show any significant contribution at this energy while the Fe $K$ edge shows peak A.

In the case of the $R$Fe$_2$ compounds in which $R$ is a magnetic rare earth, the Fe $K$-edge XMCD spectra changes drastically in comparison to that of the nonmagnetic rare earth. This is illustrated in Fig. 1(c), where the Fe $K$-edge XMCD spectra of ErFe$_2$ and YFe$_2$ are compared. The amplitude of the XMCD signal of ErFe$_2$ is one order of magnitude larger than that of YFe$_2$. Moreover, the sign of the signal is the opposite to that of YFe$_2$. [For the sake of clarity we have reversed the ErFe$_2$ signal in the comparison reported Fig. 1(c)]. It should be noted that the sign of the XMCD signals is referred to the total magnetization of the system. In the case

of ErFe$_2$ the direction of the magnetization is parallel to the Er magnetic moment, that is, antiparallel to that of Fe. Consequently, the expected sign of the Fe contribution to the $K$-edge XMCD should be opposite for ErFe$_2$ and YFe$_2$, which is in agreement with the observed signs.

The main features of the Fe $K$-edge XMCD spectrum on ErFe$_2$ in Fig. 1(c) are two negative narrow peaks, B and D, respectively, located at 2 and 14 eV above the edge and a double positive peak, labeled as C$_1$ (at $E-E_0=4$ eV) and C$_2$ (at $E-E_2=10$ eV). Despite the apparent differences between the YFe$_2$ and ErFe$_2$ $K$ Fe XMCD spectra, some similarities exist between both signals. With the opposite sign, the profile of ErFe$_2$ can also be seen as a positive peak (now double peak, C$_1$ and C$_2$) emerging superimposed to a dip between 0 and 19 eV. The intensity of features B and D in ErFe$_2$ is about one order of magnitude larger than that observed in YFe$_2$ and the features extend over an energy range from 0 to 19 eV, which is twice as large as that of YFe$_2$ (from 1 to 11 eV). The enhancement of feature C is even stronger and, as a result, the very large and well separated peaks B and D are observed in the ErFe$_2$ $K$ Fe XMCD. In this way, the main difference between both Fe $K$-edge XMCD spectra is found at $E-E_0=0$ eV. The peak A, clearly seen in YFe$_2$, is depleted to near disappearance in ErFe$_2$. The enhancement and shift of the peak B toward lower energies observed in the
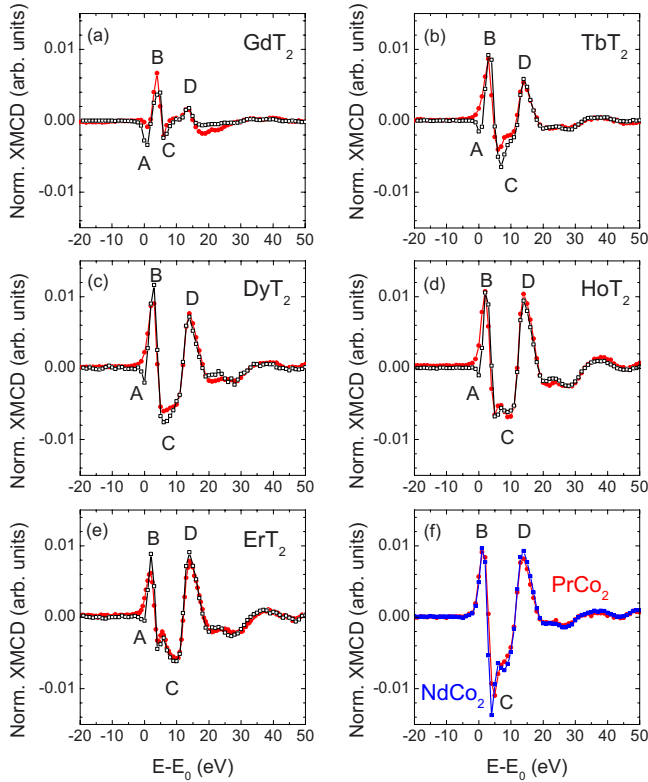
FIG. 2. (Color online) Comparison of the normalized XMCD spectra at the $K$ edge of the transition metal recorded at $T=5$ K and $H=5$ T in the case of $R\mathrm{Fe}_2$ (black, □) and $R\mathrm{Co}_2$ (red, ●) compounds for the same $R$ (Gd, Tb, Dy, Ho, and Er) [panels (a)–(e)]. Comparison of $\mathrm{NdCo}_2$ (blue, ■) and $\mathrm{PrCo}_2$ (red, ●) (panel f).

$\mathrm{ErFe}_2$ spectrum, may be the cause for the apparent depletion of the peak A, which would be the result of the overlap of the A and B peaks.

A similar situation is found when comparing the Co $K$-edge XMCD of $\mathrm{Lu}(\mathrm{Al}_{0.1}\mathrm{Co}_{0.9})_2$ and $\mathrm{ErCo}_2$ [see Fig. 1(d), here the signal of $\mathrm{ErCo}_2$ has been reversed]. Despite the apparent differences between the $\mathrm{Lu}(\mathrm{Al}_{0.1}\mathrm{Co}_{0.9})_2$ and $\mathrm{ErCo}_2$ $K$ Co XMCD spectra, some similarities exist between both signals. Reversing the sign of $\mathrm{ErCo}_2$, both profiles can be seen as a positive peak C (double peak in $\mathrm{ErCo}_2$) emerging superimposed to a dip. The intensity of features B and D in $\mathrm{ErCo}_2$ is about one order of magnitude larger than that observed in $\mathrm{Lu}(\mathrm{Al}_{0.1}\mathrm{Co}_{0.9})_2$ and they extend over a energy range (from 0 to 19 eV) twice as large as that of $\mathrm{YFe}_2$ (from 1 to 11 eV). The enhancement of the feature C is even stronger and, as a result, the very large and well separated peaks B and D are observed in the $\mathrm{ErCo}_2$ $K$ Co XMCD.

In addition, one can also observe that the Co $K$ edge of $\mathrm{ErCo}_2$ is similar to the Fe $K$ edge of $\mathrm{ErFe}_2$. This match between $\mathrm{ErFe}_2$ and $\mathrm{ErCo}_2$ is not a particular case, but a common result for the $RT_2$ series. This is illustrated in Fig. 2, where the comparison between the Fe and Co $K$-edge XMCD signals is shown for the $RT_2$ compounds with the same rare earth. The main difference between the $K$ Fe and $K$ Co XMCD spectra lies at the threshold region. While the Fe compounds show a negative A peak at $E-E_0=0$, it is absent in the Co series. This difference is a common characteristic for all the $RT_2$ pairs.

The dramatic change in the spectral profile observed when a magnetic rare earth enters the $RT_2$ compounds cannot be explained in terms of the modification of the magnetic properties of the transition metal sublattice. In the $R\mathrm{Fe}_2$ series, the iron atoms bears a stable moment ($\mu_{\mathrm{Fe}} \sim 1.5\mu_B$), independently of $R$ being magnetic or not.[41] Hence, the differences between the spectra of $\mathrm{YFe}_2$ and $\mathrm{ErFe}_2$ [Fig. 1(c)] cannot be accounted for in terms of differences in the magnetism of the Fe sublattice. A similar situation is found in the comparison between the Co $K$-edge XMCD of $\mathrm{Lu}(\mathrm{Al}_{0.1}\mathrm{Co}_{0.9})_2$ and $\mathrm{ErCo}_2$ [Fig. 1(d)]. In the $R\mathrm{Co}_2$ series, when $R$ is magnetic, a Co moment, $\mu_{\mathrm{Co}} \sim 0.8\mu_B$ is induced. The magnetic order of the d subsystem is due to the effect of the molecular field created by the $R$ moments and acting on the Co sites.[42–45] The substitution of Co by nonmagnetic Al in $\mathrm{YCo}_2$ and $\mathrm{LuCo}_2$ Pauli paramagnets, also induces ferromagnetic order.[36–40] In $\mathrm{Lu}(\mathrm{Al}_{0.1}\mathrm{Co}_{0.9})_2$, the Co atoms have a magnetic moment of $0.7\mu_B$. Hence, as in the Fe case, the strong differences between $\mathrm{Lu}(\mathrm{Al}_{0.1}\mathrm{Co}_{0.9})_2$ and $\mathrm{ErCo}_2$ cannot be ascribed to different values of the Co moments. In the same way, the close similarity between the XMCD signals of $R\mathrm{Fe}_2$ and $R\mathrm{Co}_2$ is not expected on the grounds of the magnetic properties of the transition-metal, Fe or Co, sublattice in these compounds.

The change in the XMCD profile depending on whether ($R$) is magnetic or not has been reported in previous works performed at the $K$ edge of the transition metal in both $R$-Fe (Refs. 26–28, 30, and 31) and $R$-Co (Refs. 29 and 46–48) intermetallic compounds. As commented on those works, such a contribution should not be unexpected because the final states ($4p$) probed in the $K$-edge absorption process are delocalized and, therefore, the influence of the rare-earth neighbors can be expected to be present through the characteristic $R$-$T$ hybridization in these intermetallics. However, what is really unexpected is that the rare-earth contribution dominates the spectra. Given that at the $T$ $K$-edge XMCD the probed atom is the transition metal one would in principle expect the main contribution to be related to the magnetism of the transition metal. Here, in the direct comparison of $R\mathrm{Fe}_2$ and $R\mathrm{Co}_2$ spectra, it can be seen that $\mathrm{XMCD}_R$ totally dominates both the amplitude and the spectral shape of these spectra to the extent that the Fe and Co contributions are completely masked.

In previous works[26–28,30,31,49] we have discussed that, in $R$-$T$ intermetallics with $R$ and $T$ magnetic, the transition metal contributes to the rare-earth $L$-edges XMCD spectra and, conversely, there is a non-negligible contribution of the rare earth to the $K$-edge XMCD spectra of the transition metal. As a result, when probing the delocalized $R(5d)$ or $T(4p)$ states, XMCD is a simultaneous fingerprint of the magnetic contributions coming from the different elements in the material. In particular, we have proposed that the XMCD signal corresponds to the addition of two contributions, one of $T$ origin, $\mathrm{XMCD}_T$, and other of rare-earth origin, $\mathrm{XMCD}_R$: $\mathrm{XMCD}=\mathrm{XMCD}_T+\mathrm{XMCD}_R$. This procedure is a simple extension of the two-magnetic sublattice model used to account for the magnetization of $R$-$T$ intermetallics.[50] In this model it is assumed that: (i) the total magnetization of the $R$-$T$ compounds is the addition of the magnetization of the transition-metal and the rare-earth sublattices and (ii) the contribution of the transition-metal sublattice to the magne-
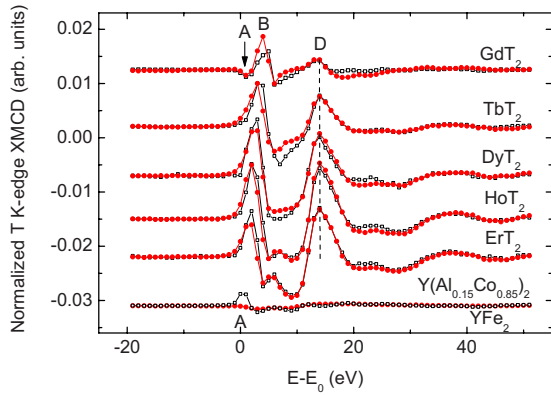
FIG. 3. (Color online) Comparison of the normalized Co $K$-edge XMCD spectra in $R$Co$_2$ (red, ●) and those of Fe $K$ edge in $R$Fe$_2$ (black, □) after subtraction of the Y(Al$_{0.15}$Co$_{0.85}$)$_2$ and YFe$_2$ spectrum, respectively ($T = 5$ K and $H = 5$ T). For the sake of clarity the spectra have been vertically shift. The spectra of YFe$_2$ and Y(Al$_{0.15}$Co$_{0.85}$)$_2$ used in the subtraction are plotted in the same scale for the sake of completeness (see text for details).

tization is identical to that of Y-$T$ (or Lu-$T$) compound. Here, we have assumed that the contribution of the $T$ sublattice, XMCD$_T$, corresponds to the XMCD signal of YFe$_2$ and Y(Al$_{0.15}$Co$_{0.85}$)$_2$ in the case of the $R$Fe$_2$ and $R$Co$_2$ compounds, respectively. For each compound in the $RT_2$ series, the subtraction of this XMCD$_T$ contribution to the recorded XMCD allows to extract the magnetic contribution coming from the rare-earth sublattice. The result of this subtraction is reported in Fig. 3. As shown in this figure, the difference previously observed in Fig. 2 at the threshold region (A peak) between the Fe and Co XMCD spectra has been suppressed after subtracting the XMCD$_T$ contribution. This result confers validity to our hypothesis asserting that after the XMCD$_T$ subtraction the obtained signal corresponds to the contribution of the rare earth and demonstrates that despite the transition metal is probed by the $K$-edge absorption, the main contribution to the XMCD spectra comes from the rare-earth counterpart in the case of the $RT_2$ compounds: XMCD$_R$ fully dominates the amplitude and spectral shape of the XMCD signal recorded at the $T$ $K$ edge.

In addition, it should be noted that for a given rare earth, the intensity of peak D matches perfectly for the $R$Fe$_2$ and the $R$Co$_2$ compounds in both the measured XMCD and the extracted XMCD$_R$ contributions. The comparison of several $R$Fe$_2$ compounds had earlier shown that, at this energy region, the XMCD spectra corresponding to nonmagnetic rare-earth compounds do not have any significant contribution[30,31] (Fig. 3). The match between $R$Fe$_2$ and $R$Co$_2$ confirms that both XMCD$_T$ and XMCD$_R$ contribute to the threshold region while for energies above ∼10 eV (i.e., peak D), the XMCD signal is exclusively due to the rare-earth sublattice.

### B. Temperature dependence

Trying to get a deeper insight into the origin of the XMCD$_R$ contribution and how it relates to the magnetic state of the rare earth, we have analyzed the thermal dependence of the $T$ $K$-edge XMCD of four different $R$(Al$_{1-x}T_x$)$_2$ com-

pounds. The spectra are shown in Fig. 4. As temperature varies, the shape of the Fe $K$-edge XMCD spectrum of ErFe$_2$ is slightly modified [see Fig. 4(a)]. In agreement with what one may expect the amplitude of the features C and D continuously decreases as temperature increases. On the other hand, peak A enhances as temperature increases. The enhancement of this peak is not envisaged on the basis of the modification of the Fe magnetic moment with the temperature. This anomalous behavior points out that the Fe $K$-edge XMCD signal cannot be simply explained in terms of just one contribution related to the magnetism of the Fe sublattice. By contrast, the thermal evolution of all the peaks in Fig. 4(a) can be satisfactorily explained if an extra contribution related to the magnetism of the Er sublattice is taken into account. On one hand, the thermal dependence of feature D in these $R$(Al$_{1-x}T_x$)$_2$ compounds has been shown to be mainly due to the rare earth.[31] The contribution of $T$ is negligible at this energy region. Hence, the temperature dependence of the features at high energy can be explained in terms of the decrease in the magnetization of the $R$ sublattice, $M_R$, as the temperature increases. On the other hand, an explanation to the enhancement of peak A has not been given so far. We propose that the particular behavior of the XMCD signal at the threshold region results from the addition of the two, Fe and Er, non-negligible contributions. The sign of these two contributions is opposite at the edge, being positive for Er and negative for Fe. At $T = 5$ K the contribution of Er, corresponding to a $\mu_{Er}$ close to the free ion value, is similar to the contribution from Fe and, as a consequence of the competition between the two contributions, the intensity of peak A is almost zero. As temperature increases, $\mu_{Er}$ decreases faster than $\mu_{Fe}$ and the total XMCD signal at the edge is progressively dominated by the negative Fe contribution. As a consequence, a negative peak progressively grows at the threshold region. The effect of this competition between XMCD$_R$ and XMCD$_T$ can also be observed in the thermal evolution of peak B. Although peak B is mainly dominated by the $R$ contribution, its decrease with temperature is smaller than that observed in peaks C and D.

The observed behavior is different for ErCo$_2$ and HoCo$_2$ [Figs. 4(b) and 4(d)]. In these cases, the magnetic moment of Co is induced by the rare earth.[42–45] Therefore, the magnetization of both sublattices decreases at the same rate with temperature. As a result, all the features in the XMCD spectrum of $R$Co$_2$ decrease at the same rate, as experimentally observed. A similar argument can be used to explain the observed behavior in the Er(Al$_{0.25}$Fe$_{0.75}$)$_2$ compound. Contrary to the ErFe$_2$ case, in this compound the Fe-Fe interaction is not the dominating one, but, the Fe-Er.[51] As a consequence, the magnetization of both sublattices decreases at the same rate in agreement with the fact that all the features on the spectrum undergo the same reduction.

Finally, it should be noticed that even in the paramagnetic regime, far from $T_C$, the same profile of the signals is still obtained, which indicates that the rare-earth contribution is still dominating the overall shape of the spectra. Therefore, from the study of the thermal dependence it can be concluded that not only peak D reflects $M_R$,[31] but the measured XMCD signal corresponds to the addition of two contributions one from Fe and other from $R$, whose amplitudes reflect
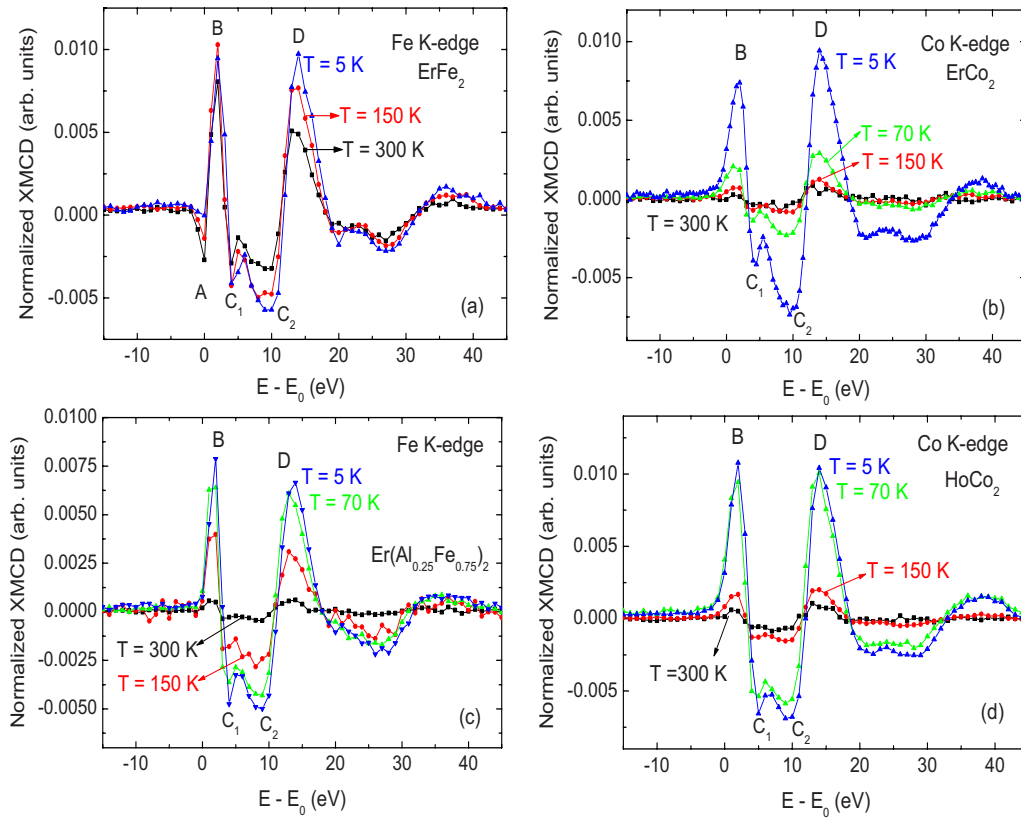
FIG. 4. (Color online). Temperature dependence of the normalized XMCD spectra recorded at the Fe $K$ edge in the case of (a) ErFe$_2$ and (c) Er(Al$_{0.25}$Fe$_{0.75}$)$_2$, and at the Co $K$ edge in (b) ErCo$_2$ and (d) HoCo$_2$: $T=5$ K (blue, ▼), 70 K (green, ▲), 150 K (red, ●), and 300 K (black, ■). All the spectra were recorded under an applied magnetic field of 5 T.

the thermal dependence of the macroscopic magnetization of the Fe and $R$ sublattices, respectively. While only XMCD$_R$ is significant at high energies, both contributions, XMCD$_R$ and XMCD$_T$, are no negligible at the threshold region.

## C. $R(Al_{1-x}T_x)_2$: Effect of Fe substitution by Al

The modification of the $T$ $K$-edge XMCD as the magnetic transition metal is substituted by Al through the $R(Al_{1-x}Fe_x)_2$ (with $R=$Gd, Tb, Dy, Ho, and Er) and Ho(Al$_{1-x}$Co$_x$)$_2$ series is illustrated in Fig. 5. This approach allows us to monitor the modification of the XMCD spectra as a function of the $R$:Fe ratio while keeping fixed the crystal structure. Despite no variation in the signals is found when Fe is changed by Co, the amplitude of the signals is detected to vary through the $R(Al_{1-x}T_x)_2$ series. As it can be seen in all the panels of Fig. 5, as the Al content increases, the spectra undergo a reduction in the intensity and a shift toward lower energy, but the spectral shape remains basically unaltered. Indeed, features B, C, and D are clearly observable even for the lowest Fe content compound ($x=0.25$). By contrast, the region of the spectrum around the threshold is more strongly modified upon increasing the Al content. The intensity of peak A is strongly reduced in such a way that for $x=0.75$ no negative peak can be observed in most of the $R(Al_{1-x}T_x)_2$ series. In fact, it is only in the Gd series, whose XMCD$_R$ is the smallest one, where the peak A is still visible for 50% Fe content.

According to magnetization and Mössbauer measurements[52–54] the magnetic moments of both, Fe and $R$ are only slightly modified as the Fe atoms are substituted by the nonmagnetic Al ones through these $R(Al_{1-x}T_x)_2$ series. Therefore, the magnetization of the $R$ sublattice remains basically constant independently on Fe content and, in the light of these data, it is concluded that the modification observed through the $R(Al_{1-x}Fe_x)_2$ series in Fig. 5 cannot be simply explained in terms of a reduction in $M_R$ and $M_{Fe}$.

The disappearance of peak A when the Fe content is decreased can be easily explained taking into account that the profile of the low energy region is determined by the competition of the $R$ and $T$ contributions. As a result, peak A is somehow hidden. Besides, as Al substitutes Fe, the features B, C and D shift toward lower energies. This shift causes an increase in the overlapping of peaks A and B resulting in the disappearance of the first spectral feature (peak A). This hypothesis, first suggested from spectra recorded on the Ho(Al$_{1-x}$Fe$_x$)$_2$ series[30] is now confirmed by a large systematic over different $R(Al_{1-x}T_x)_2$ series. Especially it is supported by the fact that in the Gd(Al$_{1-x}$Fe$_x$)$_2$ series, whose XMCD$_R$ is the smallest one, (i) the intensity of the peak A in GdFe$_2$ is significantly larger than that of DyFe$_2$, HoFe$_2$, and ErFe$_2$, while similar to that of LuFe$_2$ and YFe$_2$ and (ii) the peak A is still visible for 50% Fe content.

On the other hand, the features at higher energy are associated only to the $R$ contribution, so a different argument has to be brought concerning the modification of peaks B, C, and
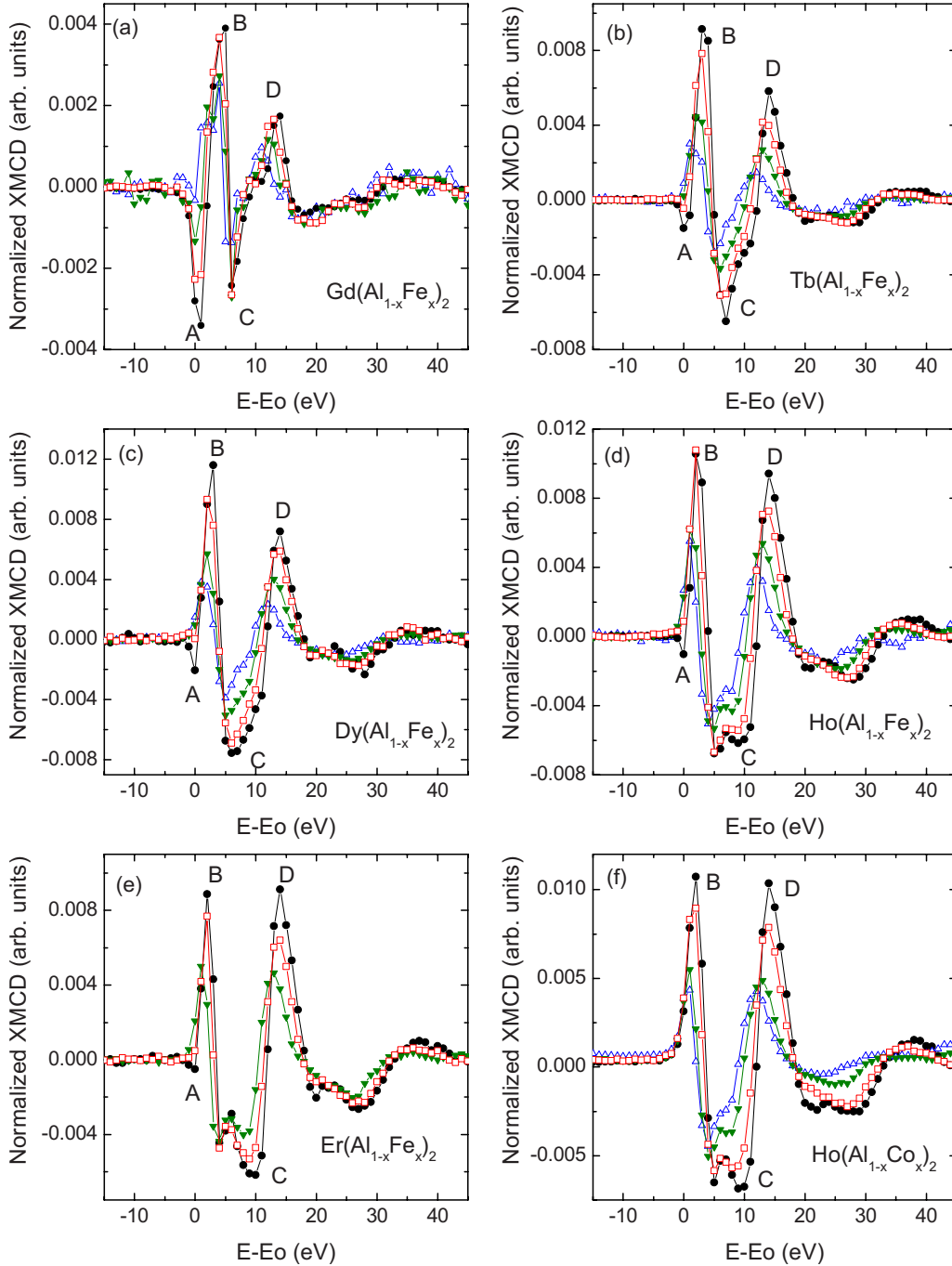
FIG. 5. (Color online) Comparison of the normalized Fe $K$-edge XMCD spectra recorded at $T=5$ K and $H=5$ T in the $R(Al_{1-x}Fe_x)_2$ series with $x=1$ (black, ●), 0.75 (red, □), 0.50 (green, ▼), and 0.25 (blue, △). Panel (f): similar comparison is shown at the Co $K$-edge in the case of the $Ho(Al_{1-x}Co_x)_2$ series.

D. In a previous study performed at the $L_2$-edge XMCD of the rare earth in the $RFe_2$ series,[28,49] we have shown that the $R$ $L_2$-edge XMCD spectra can be described as made up of two different contributions, $XMCD_R$ and $XMCD_T$. $XMCD_R$ emerges as a consequence of the polarization of the 5$d$ states by the $R(4f)$ ones through an intra-atomic exchange, and $XMCD_T$ emerges due to the $T(3d)$ states through the $T(3d)$-$R(5d)$ hybridization. Moreover, for the $R$ $L$-edges spectra it was found that the intensity of the $XMCD_T$ contribution depends not only on the magnetization of the $T$ sub-lattice but also on the specific $R$ element in the $RT_2$ series. That is, for a fixed value of the magnetization of the transition metal, the intensity of $XMCD_T$ has the same dependency on the specific $R$ as the $n_{RT}$ molecular field coefficients, which account for the strength of the interaction between the two magnetic sublattices. This pointed out that both magnitudes had a common origin. This result at the $L_{2,3}$ edges of the rare earth, led us to investigate if the observed reduction in the $R$ contribution at the $K$ edge of the transition metal is related to the strength of the $R$-$T$ exchange interaction. In

TABLE I. Magnetic parameters of the $R(Al_{1-x}Fe_x)_2$ compounds: $M$ is the magnetization measured at $T$ $=5$ K and $H=5$ kOe and $T_C$ is the Curie temperature obtained as the inflection point of the $M(T)$ curves recorded at $H=1$ kOe.

| Sample | $M$ ($\mu_B$/f.u.) | $T_C$ (K) | Sample | $M$ ($\mu_B$/f.u.) | $T_C$ (K) |
|---|---|---|---|---|---|
| YFe$_2$ | 2.87 | 541 | Y(Al$_{0.15}$Co$_{0.85}$)$_2$ | 0.38 | 22 |
| Y(Al$_{0.25}$Fe$_{0.75}$)$_2$ | 0.60 | 50 | | | |
| Y(Al$_{0.50}$Fe$_{0.50}$)$_2$ | 0.22 | PM | | | |
| Y(Al$_{0.75}$Fe$_{0.25}$)$_2$ | 0.14 | PM | | | |
| | | | PrCo$_2$ | 3.37 | 40 |
| | | | NdCo$_2$ | 3.68 | 100 |
| GdFe$_2$ | 3.91 | 793 | GdCo$_2$ | 5.00 | 400 |
| Gd(Al$_{0.25}$Fe$_{0.75}$)$_2$ | 4.92 | 420 | | | |
| Gd(Al$_{0.50}$Fe$_{0.50}$)$_2$ | 5.64 | 265 | | | |
| Gd(Al$_{0.75}$Fe$_{0.25}$)$_2$ | 6.48 | 135 | | | |
| TbFe$_2$ | 4.79 | 653 | TbCo$_2$ | 6.32 | 235 |
| Tb(Al$_{0.25}$Fe$_{0.75}$)$_2$ | 6.09 | 354 | | | |
| Tb(Al$_{0.50}$Fe$_{0.50}$)$_2$ | 6.04 | 190 | | | |
| Tb(Al$_{0.75}$Fe$_{0.25}$)$_2$ | 6.54 | 90 | | | |
| DyFe$_2$ | 6.45 | 628 | DyCo$_2$ | 7.46 | 150 |
| Dy(Al$_{0.25}$Fe$_{0.75}$)$_2$ | 6.56 | 280 | | | |
| Dy(Al$_{0.50}$Fe$_{0.50}$)$_2$ | 6.36 | 130 | | | |
| Dy(Al$_{0.75}$Fe$_{0.25}$)$_2$ | 6.04 | 60 | | | |
| HoFe$_2$ | 6.54 | 606 | HoCo$_2$ | 7.98 | 78 |
| Ho(Al$_{0.25}$Fe$_{0.75}$)$_2$ | 7.26 | 214 | | | |
| Ho(Al$_{0.50}$Fe$_{0.50}$)$_2$ | 7.63 | 85 | | | |
| Ho(Al$_{0.75}$Fe$_{0.25}$)$_2$ | 7.29 | 40 | | | |
| ErFe$_2$ | 5.57 | 582 | ErCo$_2$ | 7.15 | 32 |
| Er(Al$_{0.25}$Fe$_{0.75}$)$_2$ | 6.38 | 140 | | | |
| Er(Al$_{0.50}$Fe$_{0.50}$)$_2$ | 6.39 | 60 | | | |
| LuFe$_2$ | 2.86 | 582 | Lu(Al$_{0.1}$Co$_{0.9}$)$_2$ | 1.16 | 90 |
| Lu(Al$_{0.25}$Fe$_{0.75}$)$_2$ | 0.70 | 60 | | | |
| Lu(Al$_{0.50}$Fe$_{0.50}$)$_2$ | 0.23 | PM | | | |

these systems, as aluminum substitutes the transition metal, the rare-earth moments remain close to their free-ion values and the magnetization of the $R$ sublattice does not change significantly, but the $R$-$T$ exchange is progressively reduced as inferred from the marked reduction in $T_C$ (in Table I) and their related molecular field coefficients, $n_{RT}$.[51] Therefore, the modification of the spectra with Al (Fe) content indicates that the $R$ contribution to the $T$ $K$-edge XMCD not only reflects the magnitude of the rare-earth sublattice magnetization [of the $R(4f)$ moment], but is also related to the strength of the magnetic interaction between the two sublattices. Although further investigation is required to get a precise quantitative characterization, this suggests that the XMCD$_R$ signal can be described in terms of a "molecular-fieldlike" model.

### D. Extension to other $R$-$T$ intermetallics

In order to verify that these results are not a particularity of the Laves phases but a general result in $R$-$T$ intermetallics,

we have compared the XMCD of the $R$Fe$_2$ series with those of the $R_6$Fe$_{23}$ and $R$Fe$_{11}$Ti compounds. This comparison is exemplified in the case of Ho-Fe alloys in Fig. 6. As shown in the figure, the three Ho-Fe alloys show the same large B, C, and D features, indicating the presence of XMCD$_{Ho}$. The amplitude and the width of the XMCD signals increase in the direction HoFe$_{11}$Ti $\rightarrow$ Ho$_6$Fe$_{23}$ $\rightarrow$ HoFe$_2$. In addition, in a similar fashion to that observed for the Al-substituted $R(Al_{1-x}T_x)_2$ series, the peak B moves toward lower energy as the $R$:Fe ratio increases so that the rare-earth sublattice increasingly affects the peak A.

All the XMCD signals in Fig. 6 correspond to saturation conditions. Under these conditions the magnetic moment of Ho is close to its free-ion value: $\mu_{Ho}=10\mu_B$ (Refs. 32, 41, 50, and 55–57) and the magnetic moment of Fe is roughly constant, $\mu_{Fe} \sim 1.5\mu_B$.[27,28,32,49] On the other hand, the number of $R$ neighboring atoms surrounding the absorbing Fe (and the magnetization of the rare-earth sublattice $M_R$ relative to the magnetization of the Fe sublattice $M_T$) increases in the direction HoFe$_{11}$Ti $\rightarrow$ Ho$_6$Fe$_{23}$ $\rightarrow$ HoFe$_2$. HoFe$_2$ has a
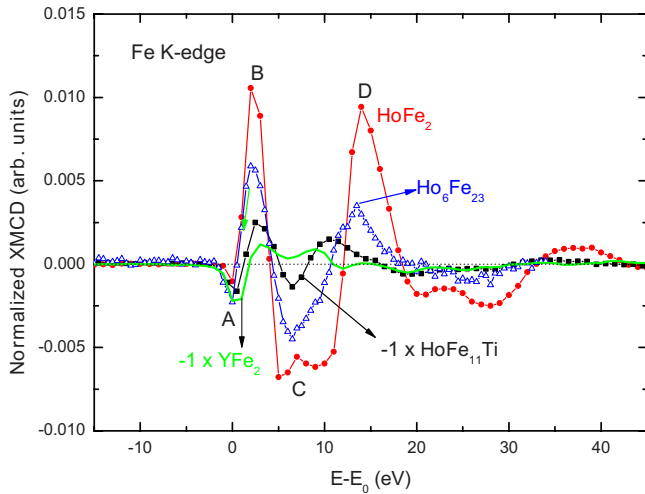
FIG. 6. (Color online) Comparison of the normalized Fe $K$-edge XMCD spectra in the case of HoFe$_2$ (red, ○), Ho$_6$Fe$_{23}$ (blue, △), HoFe$_{11}$Ti (black, ■), and YFe$_2$ (green, solid line). The spectra of FeYFe$_2$ and HoFe$_{11}$Ti have been multiplied by −1 to refer to the same direction of the Fe magnetization. All the spectra were recorded at magnetization saturation conditions.

much higher $R$ content (ratio: 1:2, average number of $R$ nearest neighbors to one absorbing $T$:6) than the Ho$_6$Fe$_{23}$ (ratio: 6:23, $Rnn$: 3.4) and HoFe$_{11}$Ti (ratio 1:11, $Rnn$: 1.7) compounds. Because the intensity of the $T$ $K$-edge XMCD in Laves compounds was larger than that observed in earlier works on the 2:14 and 1:11 series, we have recently suggested that XMCD$_R$ is also related to the number of $R$ neighbors.[30] The comparison shown in Fig. 6 is a direct proof of this. The comparison in Fig. 6 also shows that the conclusions drawn from the Laves phases compounds can be extended to other $R$:$T$ intermetallic systems.

### E. XMCD$_R$ as a function of $R$: Relationship between XMCD$_R$ and $L_{4f}$

So far we have identified the rare-earth contribution to the $T$ $K$-edge XMCD signal and monitored how it changes with temperature and $R$:Fe ratio, finding a relationship between this contribution and both the strength of the $R$-$T$ interaction and the value of the magnetization of the rare earth. However, regarding the dependence of XMCD$_R$ on $M_R$, it has to be mentioned that in all the cases, the comparisons have been done for a fixed rare earth. As a final comparison, we study how the XMCD$_R$ changes when everything is fixed but the rare earth itself. Back to Fig. 2, it can be clearly observed that, although the profile is roughly the same for all the rare earths, the details of amplitude and width vary from one $R$ to another. Can these differences be explained in terms of variations in the value of $n_{RT}$ or in $M_R$? To answer this question we have monitor the $R$ dependence by integrating the spectra in the region of energy where XMCD$_T$ is negligible, that is, in the region corresponding to peak D. The values of this integration for the $RT_2$ compounds (including the light $R$ Laves phases PrCo$_2$ and NdCo$_2$) are compared in Fig. 7(a) to the $R$ dependence of $M_R$. As it can be observed, both quan-
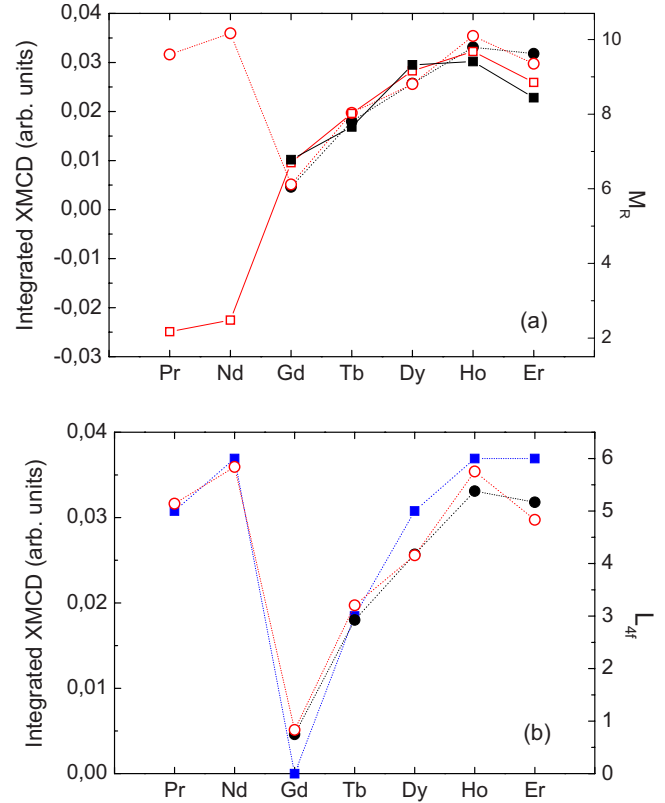


FIG. 7. (Color online) (a) Comparison of the integrated Fe $K$-edge (black, ●) and Co $K$-edge (red, ○) XMCD signals and the rare-earth magnetic moments obtained from macroscopic magnetization data, $M_R$, in $R$Fe$_2$(black, ■) and $R$Co$_2$ (red, □). (b) Comparison of the integrated Fe $K$-edge (black, ●) and Co $K$-edge (red, ○) XMCD signals and the $R(4f)$ orbital moment $L_{4f}$ (blue, ■).

tities show the same trend if only the heavy rare earth is considered. However, no agreement can be observed when the light rare earth are included in the comparison. In the same way, although it has been experimentally observed that the $R$-$T$ exchange is larger for the light $R$ than for the heavy $R$,[50] this is not enough to overcome the small magnitude of the light rare-earth magnetic moments derived from magnetization (not shown).

This indicates that the hypothesis stating that XMCD$_R$ varies as $n_{RT}xM_R$ is not correct enough and some extra argument has to be considered to explain the origin of the $R$ contribution in the $T$ $K$-edge XMCD spectrum of $R$-$T$ intermetallics. According to Igarashi and Hirai,[19,20] the XMCD of the transition metal is due to the orbital moment of the $4p$ states on the core-hole site. Furthermore, this orbital moment is mainly induced by the orbital moment of the $3d$ states on the neighboring sites through the $p$-$d$ hybridization. Then, there is a strong correlation between the behavior of the XMCD spectra and the orbital moment density of the $3d$ states. On different grounds Guo has also shown that the orbital polarization correction significantly increases the orbital moment and the magnitude of the $K$ magnetic circular dichroism.[58,59] Therefore, the $K$-edge XMCD spectrum probes the $p$-projected orbital magnetization density of unoccupied states. The results of Guo are consistent with the findings of Igarashi and Hirai showing that the $K$-edge

XMCD (i.e., the $4p$ orbital moment) is caused mainly by the spin-orbit coupling of the $3d$ states through $4p$-$3d$ hybridizations. These and other works,[19–23,58] showing the relationship between the XMCD and the $3d$ orbital density of unoccupied states assumed that the only contribution to the $T$ $K$-edge XMCD signals comes from the $T$ absorbing atom. The presence of an extra contribution coming from other magnetic atoms in the compound different from the absorbing atom was not taken into consideration. Here, we have taken into mind these previous results to get a deeper insight into the origin of the so large rare-earth contribution to the $T$ $K$-edge XMCD in the $R$-$T$ intermetallics. Thus, we have considered the orbital angular moment of the $4f$ shell ($L_{4f}$) instead of the total magnetization of the rare-earth sublattice in the comparison. As shown in Fig. 7(b), there is a good agreement between $\text{XMCD}_R$ and $L_{4f}$, which supports that the extra rare-earth contribution to the $T$ $K$-edge XMCD has an orbital origin, and that its magnitude is related to $L_{4f}$. That is, this result suggests that it is only the orbital magnetic moment instead of the total moment that polarizes the $T(4p)$ band giving rise to $\text{XMCD}_R$.

In a first approximation, the relationship between $\text{XMCD}_R$ and $L_{4f}$ can be easily accounted for in terms of a naïve picture of the polarization transmission and the strong $R$-$T$ hybridization that determines the magnetic properties of the $R$-$T$ intermetallics. Due to the intra-atomic $R(4f)$-$R(5d)$ coupling, the $R(4f)$ electrons induce an orbital polarization on the $5d$ states that is proportional to the orbital moment of the $R(4f)$ electrons. In turn, because of their delocalized nature and the existence of the $T$-$R$ hybridization, the $R(5d)$ states induce an orbital polarization on the $T(4p)$ states that is proportional to the orbital moment of the $R(4f)$ electrons. The main divergence from the general good agreement in Fig. 7(b) is found for Gd: $\text{XMCD}_{Gd}$ is not zero for $GdFe_2$ and $GdCo_2$, whereas Gd bears no orbital moment at the $4f$ shell. The fact that the Gd compounds exhibit a nonzero signal suggests that the observed rare-earth contribution to the XMCD does not merely reflects the orbital angular moment of the $4f$ shell. To this respect, it should be noted that Belorizky *et al.*[60,61] have shown that the spin and orbital polarization of the conduction ($5d$) electrons are not simply proportional to the orbital and spin moments of the rare-earth $4f$ electrons and that their expectation values depends on the total angular moment $J$ of the $4f$ shell. This result may account by for the small, yet nonzero, contribution observed for the Gd compounds.

Finally, it is worth to notice that the relationship between $\text{XMCD}_R$ and $L_{4f}$ (instead of $M_R$) has not been verified so far in any $R$:$T$ intermetallic other than $PrCo_2$ and $NdCo_2$. Besides, the evaluation of the $R$ dependence of $\text{XMCD}_R$ has been done taking into account only the peak D, but the value of the integral is highly dependent on the integration region. Therefore, further work involving other $R$:Fe series where the light rare-earth compounds are also available is highly desirable to get a verification of this later relationship.

## IV. SUMMARY AND CONCLUSIONS

We present here a study of the x-ray magnetic circular dichroism at the $K$ edge on the transition metal in rare-earth ($R$) transition-metal ($T$) intermetallics. The combined analysis of the Fe $K$-edge XMCD in the $R\text{Fe}_2$ compounds and the Co $K$-edge in $R\text{Co}_2$ reveals the presence of a rare-earth contribution, $\text{XMCD}_R$, to these spectra when $R$ is a magnetic rare earth. This confirms previous findings regarding the existence of a contribution coming from the rare-earth atoms (through the $R$-$T$ hybridization) even when the $T$ atoms are being probed. In the case of the Laves phases we find additionally that this contribution is so large that dominates the overall shape and sign of the $T$ $K$-edge XMCD. In fact, for a given $R$, the intensity and the shape of the XMCD signals in $R\text{Fe}_2$ and $R\text{Co}_2$ are almost the same despite the magnitude of the Co $3d$ magnetic moment is quite different from that of Fe in these isostructural compounds.

The study of the temperature dependence of the $T$ $K$-edge XMCD signals demonstrate that the overall XMCD signal corresponds to the addition of the Fe and $R$ contributions, whose amplitudes reflect the thermal dependence of the macroscopic magnetization of the Fe and $R$ sublattices, respectively. On the other hand, the study of $\text{XMCD}_R$ as a function of the rare earth itself shows a good agreement between $\text{XMCD}_R$ and $L_{4f}$. This latter result suggests that the rare-earth contribution to the $T$ $K$-edge XMCD has an orbital origin and that its magnitude is most likely related to $L_{4f}$ instead of $M_R$.

Moreover, despite no variation in the signals is found when Fe is changed by Co, the amplitude of the signals decreases as Fe or Co are diluted by nonmagnetic Al. Aluminum substitution does no affect the magnitude of the individual $\mu_T$ and $\mu_R$ magnetic moments but strongly reduces the magnetic interaction between the two sublattices. This result suggest a correlation between $\text{XMCD}_R$ and the strength of the $R$-$T$ magnetic interaction.

In summary, our results point out that $\text{XMCD}_R$ shows a dependence on the magnitude of the magnetic moment of the rare earth (most likely on $L_{4f}$), the number of $R$ neighbors around the absorbing $T$ atom and the strength of the $R$-$T$ interaction, suggesting that its behavior can be accounted for in terms of a molecular fieldlike (with $B_{RT} \propto n_{RT} L_R$) model.

[1] *X-ray Scattering and Absorption by Magnetic Materials*, edited by S. W. Lovesey and S. P. Collins (Oxford University Press, Clarendon, London, 1996).

[2] J. Stöhr, J. Magn. Magn. Mater. **200**, 470 (1999).

[3] J. B. Kortright, D. D. Awschalom, J. Stöhr, S. D. Bader, Y. U. Idzerda, S. S. P. Parkin, I. K. Schuller, and H.-C. Siegmann, J. Magn. Magn. Mater. **207**, 7 (1999).

[4] T. Funk, A. Deb, S. J. George, H. Wang, and S. P. Cramer, Coord. Chem. Rev. **249**, 3 (2005).

[5] G. van der Laan, B. T. Thole, G. A. Sawatzky, J. B. Goedkoop, J. C. Fuggle, J.-M. Esteva, R. Karnatak, J. P. Remeika, and H. A. Dabkowska, Phys. Rev. B **34**, 6529 (1986).

[6] G. Schütz, W. Wagner, W. Wilhelm, P. Kienle, R. Zeller, R. Frahm, and G. Materlik, Phys. Rev. Lett. **58**, 737 (1987).

[7] C. T. Chen, F. Sette, Y. Ma, and S. Modesti, Phys. Rev. B **42**, 7262 (1990).

[8] G. Schütz, R. Wienke, M. Knülle, W. Wilhelm, W. Wagner, P. Kienle, and R. Frahm, Z. Phys. B: Condens. Matter **73**, 67 (1988).

[9] G. Schütz, R. Wienke, W. Wilhelm, W. Wagner, P. Kienle, R. Zeller, and R. Frahm, Z. Phys. B: Condens. Matter **75**, 495 (1989).

[10] H. Ebert and R. Zeller, Phys. Rev. B **42**, 2744 (1990).

[11] H. Ebert, Rep. Prog. Phys. **59**, 1665 (1996).

[12] B. T. Thole, P. Carra, F. Sette, and G. van der Laan, Phys. Rev. Lett. **68**, 1943 (1992).

[13] P. Carra, B. T. Thole, M. Altarelli, and X. Wang, Phys. Rev. Lett. **70**, 694 (1993).

[14] H. Ebert, B. Drittler, P. Strange, R. Zeller, and B. L. Gyorffy, in *The Effects of Relativity in Atoms, Molecules and the Solid State*, edited by I. P. G. S. Wilson and B. L. Gyorffy (Plenum, New York, 1991).

[15] H. Ebert, P. Strange, and B. L. Gyorffy, J. Appl. Phys. **63**, 3055 (1988).

[16] G. Schütz and H. Wienke, Hyperfine Interact. **50**, 457 (1989).

[17] G. Schütz, R. Frahm, R. Wienke, W. Wilhelm, W. Wagner, and P. Kienle, Rev. Sci. Instrum. **60**, 1661 (1989).

[18] S. Stähler, G. Schütz, and H. Ebert, Phys. Rev. B **47**, 818 (1993).

[19] J.-I. Igarashi and K. Hirai, Phys. Rev. B **50**, 17820 (1994).

[20] J.-I. Igarashi and K. Hirai, Phys. Rev. B **53**, 6442 (1996).

[21] M. Takahashi and J.-I. Igarashi, Phys. Rev. B **67**, 245104 (2003).

[22] G. Y. Guo, J. Phys.: Condens. Matter **8**, L747 (1996).

[23] G. Y. Guo, Phys. Rev. B **55**, 11619 (1997).

[24] H. Ebert, Solid State Commun. **100**, 677 (1996).

[25] H. Ebert, V. Popescu, D. Ahlers, G. Schütz, L. Lemke, H. Wende, P. Srivastava, and K. Baberschke, Europhys. Lett. **42**, 295 (1998).

[26] J. Chaboy, H. Maruyama, L. M. García, J. Bartolomé, K. Kobayashi, N. Kawamura, A. Marcelli, and L. Bozukov, Phys. Rev. B **54**, R15637 (1996).

[27] J. Chaboy, M. A. Laguna-Marco, M. C. Sánchez, H. Maruyama, N. Kawamura, and M. Suzuki, Phys. Rev. B **69**, 134421 (2004).

[28] M. A. Laguna-Marco, J. Chaboy, and H. Maruyama, Phys. Rev. B **72**, 094408 (2005).

[29] J. P. Rueff, R. M. Galéra, C. Giorgetti, E. Dartyge, C. Brouder, and M. Alouani, Phys. Rev. B **58**, 12271 (1998).

[30] M. A. Laguna-Marco, J. Chaboy, C. Piquer, H. Maruyama, N. Kawamura, and M. Takagaki, J. Magn. Magn. Mater. **316**, e425 (2007).

[31] J. Chaboy, M. A. Laguna-Marco, C. Piquer, R. Boada, H. Maruyama, and N. Kawamura, J. Synchrotron Radiat. **15**, 440 (2008).

[32] *A New Insight into the Interpretation of the T K-Edge and R L$_{2,3}$-Edges XMCD Spectra in R-T Intermetallics*, edited by M. A. Laguna-Marco (Prensas Universitarias de Zaragoza, Zaragoza, 2007).

[33] J. F. Cannon, D. L. Rpbertson, and H. T. Hall, Mater. Res. Bull. **7**, 5 (1972).

[34] H. Maruyama, J. Synchrotron Radiat. **8**, 125 (2001).

[35] M. Suzuki, N. Kawamura, M. Mizumaki, A. Urata, H. Maruyama, S. Goto, and T. Ishikawa, Jpn. J. Appl. Phys., Part 2 **37**, L1488 (1998).

[36] K. Yoshimura and Y. Nakamura, Solid State Commun. **56**, 767 (1985).

[37] T. Sakakibara, T. Goto, K. Yoshimura, M. Shiga, and Y. Nakamura, Phys. Lett. A **117**, 243 (1986).

[38] T. Sakakibara, T. Goto, K. Yoshimura, and K. Fukamichi, J. Phys.: Condens. Matter **2**, 3381 (1990).

[39] I. Gabelko, R. Levitin, A. Markosyan, V. Silant'ev, and V. Snegirev, J. Magn. Magn. Mater. **94**, 287 (1991).

[40] T. Yokoyama, H. Saito, K. Mainishima, T. Goto, and H. Yamada, J. Phys.: Condens. Matter **13**, 9281 (2001).

[41] E. Burzo, A. Chelkowski, and H. R. Kirchmayr, in *Compounds Between Rare Earth Elements and 3d, 4d or 5d Elements*, Landolt-Börnstein New series, Group III Vol. 19d2, edited by H. P. J. Wijn (Springer-Verlag, Berlin, 1990).

[42] J. J. M. Franse and R. J. Radwanski, in *Handbook on Magnetic Materials*, edited by K. H. J. Buschow (Elsevier Science, Amsterdam, 1993), Vol. 7, Chap. 5.

[43] N. H. Duc and P. E. Brommer, in *Handbook of Magnetic Materials*, edited by K. H. J. Buschow (Elsevier Science, Amsterdam, 1999), Vol. 12, Chap. 3.

[44] N. H. Duc and T. Goto, in *Handbook on the Physics and Chemistry of Rare Earths*, edited by K. A. Gschneidner, Jr. and L. Eyring (Elsevier Science, Amsterdam, 1999) Vol. 26, Chap. 171.

[45] E. Gratz and A. S. Markosyan, J. Phys.: Condens. Matter **13**, R385 (2001).

[46] N. Ishimatsu, S. Miyamoto, H. Maruyama, J. Chaboy, M. A. Laguna-Marco, and N. Kawamura, Phys. Rev. B **75**, 180402(R) (2007).

[47] J. Chaboy, M. A. Laguna-Marco, H. Maruyama, N. Ishimatsu, Y. Isohama, and N. Kawamura, Phys. Rev. B **75**, 144405 (2007).

[48] J. Herrero-Albillos, D. Paudyal, F. Bartolomé, L. M. Garcia, V. K. Pecharsky, K. A. Gschneidner, Jr., A. T. Young, N. Jaouen, and A. Rogalev, J. Appl. Phys. **103**, 07E146 (2008).

[49] M. A. Laguna-Marco, J. Chaboy, and C. Piquer, Phys. Rev. B **77**, 125132 (2008).

[50] J. F. Herbst, Rev. Mod. Phys. **63**, 819 (1991).

[51] In the case of the binary $R$Fe$_2$ phases, the molecular field coefficients can be obtained following the standard procedure for $R$-Fe intermetallic compounds [see, for example, K. H. J. Buschow, in *Supermagnets: Hard Magnetic Materials*, edited by G. J. Long and F. Grandjean, (Kluwer, Dordrecht, 1991)]. In these systems the magnetic behavior of the Fe sublattices is assumed to be basically independent on the rare earth being magnetic or not, as inferred from the values of $T_C$ and $M(H)$. Then, the $n_{FeFe}$ coefficient can be derived from the value of the Curie temperature in the Y-Fe or Lu-Fe compounds, $T_{Fe}$, and the $n_{RFe}$ coefficient from the value of $\sqrt{T_C(T_C - T_{Fe})}$. By contrast, in the diluted

$R(Al_{1-x}Fe_x)_2$ compounds, the behavior of the Fe sublattices varies depending on $R$ being magnetic or not. In particular, $Y(Al_{1-x}Fe_x)_2$ and $Lu(Al_{1-x}Fe_x)_2$ do not present long-range order for $x < 0.75$, whereas, when $R$ is magnetic, there is long-range order and the magnetic moment of Fe presents a value similar to that in the binary $RFe_2$ compounds. From here it is concluded that the long-range order in this compounds is due to the $R$-Fe interaction. To some extent, this is a similar situation to that found for the $RCo_2$ series, where the order in the Co sublattice is induced by the magnetic $R$ atoms; in this case, the molecular field model yields to a $n_{RT}$ proportional to $\sqrt{T_C}$ [see, for example, E. Belorizky, M. A. Fremy, J. P. Gavigan, D. Givord, and H. S. Li, J. Appl. Phys. **61**, 3971 (1987)].

[52] C. Piquer, M. Laguna-Marco, R. Boada, F. Plazaola, and J. Chaboy, IEEE Trans. Magn. **44**, 4206 (2008).

[53] M. Besnus, A. Herr, and G. Fisher, J. Phys. F: Met. Phys. **9**, 745 (1979).

[54] M. Besnus, P. Bauer, and J. M. Genin, J. Phys. F: Met. Phys. **8**, 191 (1978).

[55] E. Burzo, Rep. Prog. Phys. **61**, 1099 (1998).

[56] K. H. J. Buschow, in *Handbook of Magnetic Materials*, edited by K. H. J. Buschow (Elsevier Science, Amsterdam, 1988), Vol. 4, Chap. 1.

[57] H. Li and J. M. D. Coey, in *Handbook of Magnetic Materials*, edited by K. H. J. Buschow (Elsevier Science, Amsterdam, 1991), Vol. 6, Chap. 1.

[58] G. Y. Guo, Phys. Rev. B **57**, 10295 (1998).

[59] M. S. S. Brooks, Physica B & C **130**, 6 (1985).

[60] E. Belorizky, J. J. Niez, and P. M. Levy, Phys. Rev. B **23**, 3360 (1981).

[61] E. Belorizky and Y. Berthier, J. Phys. F: Met. Phys. **16**, 637 (1986).